Climate change impacts on the streamflow and simulated sediment flux to Gilgel Gibe 1 hydropower reservoir – Ethiopia

T.A.Demissie[1*], F.Saathoff[2], Y.Sileshi[3], A. Gebissa[4]

[1,2,4] Institute for Environmental Engineering,
University of Rostock,
Rostock, Germany.
Justus-von-Liebig-Weg 6, 18059.

[3] Civil Engineering Department,
Addis Ababa Institute of Technology,
Addis Ababa University, Addis Ababa, Ethiopia.
yilmash@yahoo.com

*Corresponding author: tamene_adu2002@yahoo.com.

Abstract

This study examines the impact of climate change on streamflow and simulated sediment flux to the Gilgel Gibe 1 hydropower reservoir. The Soil and Water Assessment Tool (SWAT) model was used to assess the future changes in streamflow and sediment flux due to change in future precipitation and temperature. For the future period of 2041 – 2070 here after represented as 2050s the average temperature and precipitation data, simulated by the General Circulation Models ECHAM5 and HadCM3 under emission scenarios A2 and B1 were used. The predicted results show a decrease in streamflow and a drastic increase in sediment flux. This will aggravate the sedimentation problem of Gilgel Gibe 1 reservoir and reduce its storage capacity

Key words: climate change, streamflow, sediment flux, SWAT

1. Introduction

According to the IPCC 2007 fourth assessment report, the climate is expected to change mainly by an increase in anthropogenic greenhouse concentrations: global mean surface temperature increases,daily minimum temperatures are projected to increase faster than daily maximum, and the magnitude of mean precipitation generally increases with projected increase in intensity particularly in tropical regions and high latitudes. This change in climate is expected to change the regional hydrological conditions and result in a variety of impacts on water resource systems throughout the world (Zhang et al., 2007). Hydropower projects would be affected by changes in climate, particularly by regional climate change. The projected change in the mean rainfall will affect the streamflow. In addition, the projected increase in the intensity of rainfall has a significant impact on soil erosion rates (Nearing et al., 2004). Several studies have indicated the impact of climate change on soil erosion and hydrology (e.g. O`Neal et al.,2005; Zhang and Liu,2005; Zhang and Nearing,2005). The severe erosion rates from upper catchments will result in subsequent sedimentation of reservoirs reducing their storage capacity. Sedimentation due to soil erosion is the major problem threatening the lifespan of reservoirs in Ethiopia. Some preliminary studies indicate that the levels

of some reservoirs (e.g., Koka reservoir), and lakes (e.g., Alemaya, Awassa, Abaya, and Langano) in Ethiopia have decreased. The problem is so challenging that the initial water carrying capacity of the dams has been reduced (Gizaw et al.,2004). Some studies in the Gilgel Gibe basin also indicated that the challenges such as deforestation, land degradation due to poor land management practices associated with the rugged topography and the erosive rainfall in the basin pose a major threat to the lifespan of Gilgel Gibe 1 hydropower (Nebiyu,2010). The problem of sedimentation in the Gilgel Gibe 1 reservoir is a very severe. Devid et al. (2007) conducted a cross – sectional study on siltation and nutrient enrichment of Gilgel Gibe 1 and pointed out that siltation is the major problem. In addition to the Gilgel Gibe 1 hydropower plant, the power generation of the cascade hydropower plant to Gilgel Gibe 1, namely Gilgel Gibe 2 which has an installed capacity of 420MW and uses the water released from the same reservoir, will be significantly affected.

Hydropower generation plays a significant role for the sustainable economic growth of Ethiopia. The country is endowed with high hydropower potential and there is a plan of generating and exporting power to neighbouring countries. For instance, the government of Ethiopia is constructing a cascade of hydropower scheme Gibe 3 downstream of Gilgel Gibe 1 and 2. There is also a plan to construct Gibe 4 and 5 farthest downstream. These are an indication for the ongoing efforts of the government to enhance the role of hydropower in the overall development of the country. However, the potential threats to the hydropower projects such as sedimentation is not addressed. These threats might be exacerbated due to the changing climate and has not been studied.

Therefore, the objective of this study was to evaluate the potential impacts of climate change on the streamflow and simulated sediment flux to the Gilgel Gibe 1 hydropower reservoir. This is the first study that has been conducted for Gilgel Gibe1. The study result is based on hydrologic modelling under climate change and might provide an insight to planners and decision makers regarding the impact of climate change.

Several mathematical models are available to evaluate potential future implications due to the factors driving the changes. Of these, the Soil and Water Assessment Tool (SWAT) model has been employed widely to evaluate the impact of climate change on soil erosion and sediment yields (Shrestha et al.,2012). It has also been used to evaluate the impact of climate change on streamflow. For instance, Fontaine et al.(2009), Githui et al.(2009), Ficklin et al.(2009), and Li et al. (2011) used SWAT model to evaluate the impact of climate change on streamflow. Several researchers have applied the SWAT model in Ethiopia. For instance, the SWAT model was applied by Setegn et al. (2010) for the simulation of sediment yield in the Anjeni gauged catchment within the Blue Nile River basin. Mengistu and Sorteberg (2012) used the SWAT model to investigate the sensitivity of SWAT simulated streamflow to climatic changes within the Eastern Nile River basin. All the SWAT model applications in Ethiopia concentrate on the Blue Nile River Basin and none has been applied on Gibe basin in general and Gilgel Gibe basin in particular. Based on the previous experiences of SWAT model application and the acceptable results obtained in Ethiopia, the SWAT model is preferred for this study.

The SWAT model was calibrated and validated for the streamflow. Following the calibration and validation of the model, the future temperature and precipitation changes projected by ECHAM5 and HadCM3 under emission scenarios A2 and B1 were used to construct future climate series. The delta change (change factor) approach was used to develop the future climate series.

2. Study area description

The Gilgel Gibe 1 project is located in the south-western part of Ethiopia, in Oromia Regional state. The reservoir is located at $7^{o}49`52.45``N$ latitude and $37^{o}19`18.79´´E$ longitude.The project is purely a

hydropower scheme, with an installed capacity of 180MW. The reservoir has a live storage capacity of $657x10^6m^3$. The catchment area of the Gilgel Gibe basin is about $5125km^2$ at its confluence with the great Gibe River and about $4225km^2$ at the dam site. The Gilgel Gibe basin which drains in to the Gilgel Gibe 1 reservoir is located in between 7^o 19´07.15´N and 8^o12´09.49´´N latitudes and 36^o31´42.60´´ E to 37^o25`16.05´´E longitudes. The basin is generally characterised by high relief hills and mountains with an average elevation of about 1700m above mean sea level. The basin is largely comprised of cultivated land. In general terms, the Gilgel Gibe basin is characterised by a wet climate with an average annual rainfall of about 1550 mm and an average temperature of 19 ^oC. The seasonal rainfall distribution takes a uni-modal pattern with its maximum during the summer and minimum during the winter, influenced by the inter-tropical convergence zone (ITCZ). Figure 1 shows the location map of Gilgel Gibe 1 and cascade hydropower projects**.**

3. Materials and Methods

3.1.Observed weather data and spatial data

The SWAT model requires daily weather data and spatial data. The daily weather data required to run the SWAT model were obtained from the National Meteorology Agency (NMA) of Ethiopia. The daily data for rainfall , minimum and maximum temperature, wind speed and relative humidity for Jimma and Sekoru stations were obtained. These data covers a period of 26 years from 1980 to 2005.

The land use/land cover and soil data which was provided by Dr Abbaspour of Eawag (http://www.eawag.ch/index_EN) is extracted from http://www.waterbase.org/resources.html.

The land cover classes in this area include: Dryland Cropland and Pasture (CRDY, 36.68%), Grassland (GRAS, 15.56%), Savanna (SAVA,14.45%), Evergreen Forest (FOEB,22.65%), Mixed Forest (FOMI,9.92%) and Cropland/woodland mosaic (CRWO,0.74%). Soil properties for two layers, 0 – 30 cm and 30 – 100 cm depth, are also provided (Leon, 2011). The soil types in the area are nitosols.

To delineate the catchment and extract the topographic parameters a 90 m Digital Elevation Map (DEM) was obtained from the Consortium for Spatial Information (http://srtm.csi.cgiar.org).

3.2.Climate change scenario and GCM model

After evaluating the long term emissions scenarios developed in 1990 and 1992, the IPCC developed a new set of scenarios which can be used in the analysis of possible climate change, assessment of impacts, and adaptation and mitigation. The Special Report on Emission Scenarios (SRES) scenarios cover a wide range of the main deriving forces of future emissions, from demographic to technological and economic developments and they also include range of emissions of all relevant types of green house gases (GHGs) and sulphur and their deriving forces (Nakicenovic et al., 2000).

Among all the SRES scenarios are A1,A2,B1 and B2 are the widely used scenarios (Van Vuuren and O´Nell, 2006).

The A1 and B1 story-line and scenario family describes a convergent world with population growth that peaks in the middle of the century and declines there after. The A2 and B2 story line and scenario family emphasises local solutions to economic, social, and environmental sustainability projecting a more differential world. In this study, the A2 and B1 scenarios, which represent high and low GHG emission scenarios (IPCC, 2007), were adopted.

GCMs are the most advanced tools currently available for simulating the response of the global climate system to increasing greenhouse gas concentrations (www.ipcc-data.org/ddc_gcm-html). For this study, the

out puts from ECHAM5-OM developed by Max-Planck-Institut for Meteorology Germany and HadCM3 developed by UK Met.Office were used under the A2 and B1 IPCC emission scenarios.
The monthly average values of 2m surface air temperature and total precipitation for baseline period of 1971 – 2000 and the future period of 2041 – 2070 were downloaded from the World Data Center for Climate, Hamburg.
The spatial resolution of GCMs is too coarse to resolve regional hydrometeorological processes. Therefore, the raw outputs from GCM simulations are inadequate for assessing hydrologic impacts of climate change at regional scale (Hay et al., 2000). Hence, the GCM data corresponding to the grid box closest to the study area was extracted and linearly interpolated in both longitudinal and latitudinal directions to Jimma station located in the catchment. Then the delta change method (change factor) method was applied to construct future temperature and precipitation series. Delta change method is the difference between the future and the present day estimates (Raghavan et al.,2012). For this study changes are the difference between future climate projections 2041 – 2070 (2050s) and the 1971 – 2000 baseline current climate simulations. These changes were used to adjust the observed time series of temperature and precipitation. Temperature was modified by the absolute difference between the monthly future and simulated climate, where as precipitation was modified by the relative difference between the monthly future and actual simulated by the GCM. The results of the delta change method are presented in Table.1 and Table 2.

3.3 SWAT model description

SWAT is a physically based and spatially distributed model which was developed to assess the impact of management practices on water supplies and non-point source pollution in watersheds and large river basins (Arnold et al., 1998). It simulates streamflow, sediment yield , and nutrient and pesticide transport at catchment scale, on a continuous, daily time step (Neitsch et al., 2011). For modelling purposes, the watershed is delineated and divided into subbasins. The subbasins are further divided into hydrologic response units (HRUs) based on the land use, the soil types and the slope classes. The model estimates relevant hydrologic components such as surface runoff and peak rate of runoff, evapotranspiration, groundwater flow and sediment yield for each HRU unit. Since the objective of this study was to examine the streamflow and sediment flux responses to climate change, the surface runoff and sediment yield components of the SWAT was described briefly.
The land phase of the hydrologic cycle is simulated based on the water balance as Eq. (1).

$$SW_t = SW_0 + \sum_{i=1}^{t} (R_{day} - Q_{surf} - Ea - w_{seep} - Q_{gw}) \qquad (1)$$

Where: SW_t is the final soil water content (mm H_2O), SW_o is the initial soil water content in day i (mm water), t is the time (days), R_{day} is the amount of precipitation in day I (mm H_2O), Q_{surf} is the amount of surface runoff in day i (mm H_2O), Ea is the amount of evapotranspiration in day i (mm water), W_{seep} is the amount of water entering the vadose zone from the soil profile in day i (mm H_2O), and Q_{gw} is the amount of return flow in day i (mm H_2O).
To estimate surface runoff two options are available : The SCS curve number procedure of USDA Soil Conservation Service (USDA SCS, 1972) and the Green & Ampt infiltration method (Green and Ampt, 1911). In this study, the SCS curve number method was used to estimate surface runoff. The SCS curve number is determined as:

$$Q_{surf} = \frac{(R_{day} - I_a)^2}{(R_{day} - I_a + S)} \quad (2)$$

Where Q_{surf} is the accumulated runoff or rainfall excess (mm), R_{day} is the rainfall depth for the day (mm), Ia is the initial abstraction which includes surface storage, interception and infiltration prior to runoff (mm H_2O) and S is the retention parameter (mm H_2O).

The retention parameter is defined by Eq.(3).

$$S = 254\left(\frac{100}{CN} - 1\right) \quad (3)$$

Where CN is the curve number for the day. The initial abstraction, I_a, is commonly approximated as 0.2S and eqaution 2 becomes

$$Q_{surf} = \frac{(R_{day} - 0.2S)^2}{(R_{day} + 0.8S)} \quad (4)$$

The SCS curve number is a function of the soil's permeability, landuse and antecedent soil moisture conditions.

SWAT model calculates the surface erosion within each HRU with the Modified Universal Soil Loss Equation (MUSCLE) (Williams, 1975). The MUSCLE is:

$$sed = 11.8\left(Q_{surf}.q_{peak}.area_{hru}\right)^{0.56}.K_{USLE}.C_{USLE}.P_{USLE.}.LS_{USLE}.CFRG \quad (5)$$

Where: *sed* sediment yield on a given day (tons), Q_{surf} is the surface runoff volume (mm water/ha), q_{peak} is the peak runoff rate (m^3/s), $area_{hru}$ is the area of the HRU(ha), K_{USLE} is the USLE soil erodibility factor (0.013 metric ton m^2hr/(m^3.metric ton cm)), C_{USLE} is the USLE cover and management factor, P_{USLE} is the USLE support practice factor, LS_{USLE} is the USLE topographic factor and *CFRG* is the coarse fragment factor.

Sediment transport in the channel network is a function of two processes, deposition and degradation, operating simultaneously in the reach. SWAT computes the maximum concentration of sediment in the reach at the beginning of the time step. Depending on the concentration of sediment in the reach and transport capacity of the channel deposition or degradation process will occur.

the final amount of sediment in the reach is determined as:

$$sed_{ch} = sed_{ch,i} - sed_{dep} + sed_{\deg} \quad (6)$$

where sed_{ch} is the amount of suspended sediment in the reach (metric tons day−1), $sed_{ch,i}$ is the amount of suspended sediment in the reach at the beginning of the time period (metric tons day−1), sed_{dep} is the amount of sediment deposited in the reach segment (metric tons day−1), and sed_{deg} is the amount of sediment reentrained in the reach segment (metric tons day−1).

The amount of sediment transported out of the reach is calculated as:

$$sed_{out} = sed_{ch} x \frac{V_{out}}{V_{ch}} \quad (7)$$

where sed_{out} is the amount of sediment transported out of the reach (metric tons day−1), sed_{ch} is the amount of suspended sediment in the reach (metric tons day−1), V_{out} is the volume of outflow during the time step (m3/s), and V_{ch} is the volume of water in the reach segment (m^3). A detailed description of the model components can be found in (Neitsch et al.,2011).

3.4. Sensitivity analysis, calibration and validation of the SWAT model

There are several calibration and uncertainty analysis techniques common among researchers (Setegn et al., 2010). For this study, the Sequential Uncertainty FItting 2 (SUFI2) was used to calibrate and validate the SWAT model. In SUFI-2, parameter uncertainty accounts for all sources of uncertainties and it expresses the total uncertainty of the model interms of the final parameter ranges which also corresponds to the model output ranges (Abbaspour et al., 2007).

The degree to which all uncertainties are accounted for is quantified by a measure referred to as the P-factor, which is the percentage of measured data bracketed by the 95% prediction uncertainty (95PPU). Another measure quantifying the strength of a calibration/uncertainty analysis is the so-called R-factor, which is the average thickness of the 95PPU band divided by the standard deviation of the measured data. An ideal situation would lead to a P-factor of about 100% and a R-factor near zero. The average thickness of the 95PPU band (P) and the R-factor are calculated by using Eq.8 and Eq.9.

$$P = \frac{1}{n}\sum_{l=1}^{n}(Q_U - Q_L)_l \qquad (8)$$

$$R - factor = \frac{P}{\sigma_X} \qquad (9)$$

Where : n is the number of observed data points, Q_U and Q_L are the 97.5th percentiles and 2.5th percentiles of the cumulative distribution of every simulated point respectively. σ_X is the standard deviation of the measured variable Q.

Further performance of fit was quantified by the Nash-Sutcliffe-efficiency (NS) and R^2 coefficient between the observation and the final best simulation.

$$NS = 1 - \left[\frac{\sum_{i=1}^{n}(Q_i^{obs} - Q_i^{sim})^2}{\sum_{i=1}^{n}(Q_i^{obs} - Q^{mean})^2}\right] \qquad (10)$$

$$R^2 = \frac{\left[\sum_{i=1}^{n}(Q_i^{sim} - Q_{mean}^{sim})(Q_i^{obs} - Q_{mean}^{obs})\right]^2}{\sum_{i=1}^{n}(Q_i^{sim} - Q_{mean}^{sim})^2\sum_{i=1}^{n}(Q_i^{obs} - Q_{mean}^{obs})^2} \qquad (11)$$

Where: Q_i^{obs} is observed streamflow in m^3/s, Q_i^{sim} is simulated streamflow in m^3/s, and Q^{mean} mean of n values, Q_{mean}^{sim} is mean of simulated values, Q_{mean}^{obs} mean of observed values, and n number of observations.

Before applying SUFI-2 for calibration, the most sensitive parameters were identified by running the sensitivity analysis. To find the sensitive parameters Latin hypercube simulation, the One At -a- Time (LH-OAT) method was used (van Griensven et al.,2006). All the 27 flow-related parameters were considered for sensitivity analysis the most sensitive parameters are as depicted in Table 3.

The mean monthly discharge data of the period 1980 to 1992 and 1993 to 2000 were used to calibrate and validate the model. The selected period for streamflow calibration and validation was preferred as this data period was relatively free of gaps.

4. Results and discussions

4.1. Monthly and seasonal rainfall and temperature changes

For future period of the 2050s, Fig.2 shows the predicted monthly temperature change for the GCM scenarios. The graph indicates that the temperature increase for the future period of 2041 – 2070 is in the range of 1°C to 2.5°C, except for ECHAM5-A2. The ECHAM5 model under emission scenario A2 predicted a temperature increase of 3.12°C for June.

As it is shown in Fig. 3, both models and scenarios predicted a change in mean monthly rainfall within the range of -20% to 60% for all months except ECHAM5 model under A2 scenario predicting greater than 60% for the month of August.

Figure 4 shows the seasonal temperature change. The temperature increases from 1°C to 2.25 °C. ECHAM5 model predicted the temperature increase in the rainy season to be slightly greater than the dry season. However, the HadCM3 model predicted the dry season temperature to be slightly greater than the wet season. Figure 5, shows the seasonal rainfall change. The seasonal rainfall increases in the range of 2.45% to 45 % for rainy season and 11.45 % to 24% for dry season.

The increase in the rainy season rainfall predicted by the ECHAM5 model is considerably greater than the dry season increase. In the contrary, the increase in seasonal rainfall predicted by HadCM3 model for dry season is greater than that of the rainy season. The difference in the results obtained for both models under the same emission scenarios shows the unceratainty in GCM models simulations. Therefore, multiple GCMs should be used to provide a range of possible outcomes for decision makers so as to enable them to make proper decisions to safeguard the water resources projects. Generally, rainfall and temperature is expected to increase over the basin in the future period of the 2050s.

4.2. SWAT model calibration and performance evaluation

As stated in section 3.4 the model was calibrated and validated for monthly streamflow. However, it was not done for sediment yield due to the lack of data. The SUFI-2 calibration resulted in the P-factor and R-factor of 0.61 and 0.56 respectively. For measuring the goodness of fit, the NS of 0.707 and R^2 of 0.775 was obtained for calibration and the NS of 0.707 and R^2 of 0.767 for validation. Figure 6 shows the calibration and validation graphs and Table 3 shows sensitive parameters and fitted values by SUFI2.

The simulation results were considered to be good if NS $\geq$0.75, and satisfactory if $0.36 \leq NS \leq 0.75$ (Van Liew and Garbrecht, 2003). The coefficient of determination R^2 value indicates the strength of linear relationship between simulated and observed value and it ranges from 0 to 1. The higher value of R^2 indicates a better agreement. As shown in Fig.6, the simulated monthly flow closely matched the observed values for the calibration period. For the validation period, the rising limb of the hydrograph and the peak discharge is simulated well and is an acceptable value.

4.3. Impact of climate change on streamflow and simulated sediment flux.

Figure 7 shows the change in mean monthly discharge with respect to control perod of 1981 – 2000 of SWAT model simulation results due to climate change inputs of the ECHAM5 model and HadCM3 model under A2 and B1 scenarios. The SWAT model simulation for observed data of 1981 – 2000 is used as a control period for assessing the climate change impact. The ECHAM5 model inputs under both A2 and B1 scenarios predicted a decrease in discharge for all the months except August. In August, the discharge increases by 3.8% and 4.5% for A2 and B1 scenarios respectively. The model simulation results due to climate change input of the HadCM3 model under A2 scenario show an increase in discharge during May – September, with a maximum increase of 6.4% in June. Under B1 scenario, the model simulated a 2.8% increase in discharge only for August. The discharge is expected to decrease during October – April under A2 scenario with a maximum decrease of 6.1% occurring in December. The maximum decrease of 11.3% is simulated for B1 scenario and it occurrs in January.

As climate changes, the average annual streamflow is predicted to decrease within the range of 1.3% to 3.5% for the future period of 2050s. Figure 8 shows the change in annual streamflow.
Figure 9 shows the predcicted mean monthly sediment flux that slightly decreases during March – May, and increases during July – February, with the highest increase taking place in August for both emission scenarios and models. The highest increase in sediment flux coincides with an increase in discharge. It is important to note that the predicted change in sediment flux increases in contrast to predicted discharge which decreases. More than 80% of the sediment flux will be delivered to the reservoir during the months of the rainy season June – September and the following two months October and November. Figure 10 shows the mean annual sediment flux. The sediment flux due to climate change increases within the range of 12% - 22.3%. Generally, this study result indicate a decrease in predicted streamflow and an increase in predicted sediment flux for the future period of 2050s. An increase in sediment flux might be due to the predicted increase in rainfall over the catchment. An increase in temperature might also increase sediment flux. Li et al., (2011) indicated that increase in temperature as a result of global warming may increase the soil loss. The increase in soil loss from the upper catchment will increase the sediment flux to the reservoir. The predicted increase in temperature causes increased evaporation loss which in turn result in a decrease in streamflow.
Note: For Figure 7 – Figure 10, E stands for ECHAM5 and H stands for HadCM3. Followed by the future period and emission scenario.

5.Conclusions

In this study, the impact of climate change was examined on the future streamflows and simulated sediment flux to the Gilgel Gibe 1 hydropower reservoir. The future period 2050 was considered and future average temperature and precipitation data using the delta change method was constructed. Generally both the ECHAM5 and HadCM3 models predict an increase in average temperature and rainfall in the study area. The absolute monthly difference for temperature and relative difference for precipitation between the future period and baseline period was determined and superimposed on the historical (observed data) to run the calibrated and validated SWAT hydrological model. The results from the SWAT models as compared to the control period of 1981 – 2000, shows the decrease in streamflow for the 2050s. But the SWAT output results for simulated sediment flux show a drastic increase for the future period. This predicted increase in sediment flux due to climate change will exacerbate reservoir sedimentation. The sedimentation might significantly reduce the life span of the reservoir and the hydroelectric power generation. Therefore, decision makers and all concerned stakeholders should plan and implement an integrated watershed development programme in advance to alleviate the problem. In order to obtain more reliable results on future changes in streamflow and sediment flux, studies should be carried out by considering future changes in land use and other climate variables. The decrease in streamflow indicate as the government should also look in to other alternative sources of energy that might not be affected by climate change in addition to hydropower.

References

Abbaspour, K.C., Yang, J., Maximov,I.,Siber, R., Bogner, K., Mieleitner, J., Zobrist, J., Srinivasan, R.(2007). Modeling hydrology and water quality in the pre-alpine/alpine Thur watershed using SWAT, Journal of Hydrology.,333,413-430.

Arnold, J.G.,Srinivasan, R.,Muttiah, R. S., and Williams, J.R.(1998). Large Area hydrologic modelling and assessment Part I: Model development Journal of America Water Resources. Association ,.34:73-89.
Devi, R., Esubalew, T. Worku, L., Bishaw, D. and Abebe, B.(2007). Assessment of siltation and nutrient enrichment of Gilgel Gibe dam, Southwest Ethiopia. Bioresource Technology., 99, 975-979.

Ficklin, D.L., Luo, Y., Luedeling, E., and Zhang, M. (2009). Climate Change sensitivity assessment of a highly agricultural watershed using SWAT, Journal of Hydrology, 374, issues 1-2, 16-29.
Fontaine, T.A., J. F. Klassen, T. S. Cruickshank & R. H. Hotchkiss.(2001).Hydrological response to climate change in the Black Hills of South Dakota, USA, Hydrological Sciences Journal, 46:1, 27-40.
Green, W.H. and Ampt, G.A.(1911). Studies on soil physics, 1. The flow of air and water through soils. Journal of Agricultural Sciences 4:11.
Githui, F., Gitau, W., Mutua, F., and Bauwens,W.(2009). Climate change impact on SWAT simulated streamflow in western kenya, Int.J.Climatol, 29,1823-1834.DOI:10.1002/ioc.1828.
Gizaw,E., Legesse,W., Haddis, A., Deboch, D., and Birke, W.(2004).Assessment of factors contributing to eutrophication of Abasamuel water reservoir in Addis Ababa Ethiopia, Journal of Health Science, **14** (2) ,112–113.
Hay, L.E, Wilby, R.L., and Leavesley, H.H. (2000).Comparison of Delta Change and Downscaled GCM Scenarios For three mountainous basins in The United States, J. Am. Water Resour. Assoc., 36, 387-397.
IPCC-Intergovernmental Panel on Climate Change.(2007).Climate Change:AR4 synthesis report, Cambridge University Press, Cambridge.
IPCC-Intergovernmental Panel on Climate Change Data Distribution Centre,www.ipcc-data.org/ddc_gcm-html
IPCC-Intergovernmental Panel on Climate Change.(2007).Climate Change: The physical science basis.In: Solomon,S.et al.(Eds.), Contribution of Working Group I to the Fourth Assessment Report of the Intergovernmental Panel on Climate Change, Cambridge University Press, Cambridge.
Jarvis, A., Reuter, H.I., Nelson, A., and Guevara, E.(2008). Hole-filled Seamless SRTM data Version 4, International Centre for Tropical Agriculuture (CIAT), available from (http://srtm.csi.cgiar.org).
Leon, L.F. (2011). Step by Step Geo-Processing and Set-up of the Required Watershed Data for MWSWAT (MapWindow SWAT), Version 2.
Li, Y., Chen, B.M.,Wang, Z., and Peng, S.(2011). Effects of temperature change on water discharge, and sediment and nutrient loading in the lower Pearl River basin based on SWAT modelling, Hydrological Sciences Journal, 56:1, 68-83.
Mengistu, D.T., and Sorteberg, A.(2012). Sensitivity of SWAT simulated streamflow to climatic changes within the Eastern Nile River basin. Hydrol. Earth Syst. Sci., 16, 391–407, 2012. doi:10.5194/hess-16-391-2012.
Nakicenovic,N., Davidson, O., Davis, G., Grübler, A., Kram,T.,La Rovere,E.L.,Metz, B.,Morita, T., Pepper,W.,Pitcher,H., Sankovski, A., Shukla,P., Swart,R.,Watson, R., Dadi, Z.(2000). IPCC Special Report on Emissions Scenarios. Cambridge, UK. Cambridge University Press.
Nebiyu, A.(2010). The Sustainable use of Soil Resources of Gilgel Gibe dam catchment. Proceeding of the national workshop in integrated watershed Management on Gibe-Omo basin, Jimma University and Gilgel Gibe site, 39-42.

Nearing, M.A., Pruski,F.F., and O´Neal, M.R.(2004). Expected climate change impacts on soil erosion rates, a review. Journal of Soil and Water conservation 59,Number 1.
Neitsch,S.L., Arnold,J.G., Kiniry,J.,Williams, J.R.(2011). Soil and water assessment tool theoretical documentation (version 2009), Grassland, Soil and Water Research Laboratory-Agricultural Research Service Blackland Research Center-Texas AgriLife Research.
O'Neal, M.R., Nearing, M.A., Vining, R.C., Southworth, J., and Pfeifer, R.A. (2005). Climate change impacts on soil erosion in Midwest United States with changes in crop management, Catena 61: 165–184.

Production Estimates and Crop Assessment Division Foreign Agricultural Service –USDA. http://www.fas.usda.gov/pecad2/highlights/2002/10/ethiopia/baseline/eth_annual_rainfall).

Raghavan, S.V., Vu, M.T., and Liong, S.Y.(2012). Assessment of future stream flow over the Sesan catchment of the Lower Mekong Basin in Vietnam, Hydrol. Process, 26, 3661–3668. DOI: 10.1002/hyp.845.

Setegn, S.G., Srinivasan, R., Melesse, A.M., and Dargahi, B.(2010). SWAT model application and prediction uncertainty analysis in the Lake Tana basin, Ethiopia. Hydrol. Process.24,357-367 DOI:10.1002/hyp.7457.

Shrestha, B., Bebel, M.S., Maskey, S., van Griensven, A. Uhlenbrook, S., Green, A., and Akkharath, I. (2012). Impact of Climate Change on sediment yield in the Mekong River Basin: a case study of the Nam Ou Basin, Lao PDR, Hydrol. Earth Syst.Sci.Discuss, 9, 3339-3384.

USDA-SCS – United States Department of Agriculture - Soil Conservation Service.(1972. National Engineering Handbook,Section IV, Hydrology, 4-102.

van Griensven, A., Meixner, T., Grunwald, S.,Bishop, T., Diluzio, M., and Srinivasan, R.(2006). A global sensitivity analysis tool for the parameters of multi-variable catchment models, Journal of Hydrology, 324: 10-23.

Van Liew, M.W.,and Garbrecht, J.(2003).Hydrologic Simulation of the Little Washita river experimental watershed using SWAT. J. Am. Water Resour. Assoc., 39(2):413-426.

Van Vuuren, P.D., and O' Nell, B.C.(2006). The consistency of IPCC's SRES Scenarios to recent literature and recent projrctions: climatic change 75:9-46.

Waterbase.http://www.waterbase.org/download_data.html.

Williams, J.R.(1975).Sediment-yield prediction with universal equation using runoff energy factor.p.244-252.In Present and prospective technology for predicting sediment yield sources: Proceedings of the sediment-yield workshop, USDA Sedimentation Lab.,Oxford.MS,1972. ARS-S-40.

Zhang, X.C., Liu, W.Z. (2005). Simulating potential response of hydrology, soil erosion, and crop productivity to climate change in Changwu tableland region on the Loess Plateau of China, Agricultural and Forest Meteorology 131 :127–142.

Zhang, X.C., Nearing, M.A.(2005). Impact of climate change on soil erosion, runoff, and wheat productivity in central Oklahoma, Catena 61: 185–195.

Zhang, X., Srinivasan, R., Hao, F.(2007).Predicting Hydrologic Response to Climate Change in the Luohe River Basin Using the SWAT model, Transactions of the ASABE , 50(3): 901-910.

Table 1 : Changes in mean monthly, rainy season,dry season and annual average temperatures under scenarios A2 and B1, and models ECHAM5, and HadCM3 with respect to their 20th century run (20c3m) 1971 – 2000 baseline.

Period	Model	Scenario	Month												Season		
			Jan	Feb	Mar	Apr	May	Jun	Jul	Aug	Sep	Oct	Nov	Dec	Rainy	Dry	Annual
2041-2070	ECHAM5	A2	2.14	2.08	2.1	1.83	2.5	3.12	2.46	1.93	1.83	1.93	2.12	2.34	2.34	2.17	2.20
2041-2070	ECHAM5	B1	1.46	1.47	1.67	1.32	2.01	2.06	1.74	1.5	1.3	1.58	1.65	1.69	1.65	1.57	1.62
2041-2070	HadCM3	A2	2.48	2.21	2.01	2.26	2.24	2.43	2.33	2.11	2.16	2.15	2.25	2.51	2.26	2.36	2.26
2041-2070	HadCM3	B1	1.77	1.44	1.17	1.42	1.64	1.77	1.59	1.44	1.54	1.58	1.67	1.97	1.59	1.71	1.58

Table 2: Changes in mean monthly, rainy(wet) season, dry season and annual average precipitation under scenarios A2 and B1, and models ECHAM5 and HadCM3 with respect to their 20th century run (20c3m) 1971 – 2000.

Period	Model	Scenario	Month												Season		
			Jan	Feb	Mar	Apr	May	Jun	Jul	Aug	Sep	Oct	Nov	Dec	Rainy	Dry	Annual
2041-2070	ECHAM5	A2	6.6	-7.9	4	-11.8	-14.8	12.3	46.3	86.4	38.7	-14.3	-25.5	13.2	45.93	11.45	16.05
2041-2070	ECHAM5	B1	5.3	47.2	-18.6	-2.9	-5	14.1	51.2	65.9	46	-16.1	5.5	6.1	44.30	16.03	16.56
2041-2070	HadCM3	A2	2.9	34.9	52	17.1	-5.8	-1.8	5.2	11.3	4.7	-4.4	17.9	17.7	4.85	18.35	12.64
2041-2070	HadCM3	B1	24.1	19.9	41	16.8	-9.5	-9.3	2.5	11	5.6	-6.8	25.2	25.5	2.45	23.68	12.17

Note: The western half of Ethiopia in which the study area is located has two distinct seasons: the wet season from June to September and dry from November to February, with the rainfall peak occurring from July to August.
source:http://www.fas.usda.gov/pecad2/highlights/2002/10/ethiopia/baseline/eth_annual_rainfall.

Table 3: Flow-sensitive parameters and fitted values using SUFI-2

No	Sensitive parameter	Lower and Upper bound	Fitted value
1	*m-CN2	-0.2 to 0.2	-0.190
2	**v-ALPHA_BF	0 to 1	0.824
3	v-GW_DELAY	30 to 450	55.410
4	v-GW_REVAP	0 to 0.2	0.190
5	v-GWQMN	0 to 2	0.875
6	v-ESCO	0.8 to 1	0.913
7	m-SOL_AWC	-0.2 to 0.4	0.389
8	v-CANMX	0 to 100	76.250

Note:
*m-sensitive parameter shows multiply by 1+ the given fitted value.
**v-sensitive parameter shows replace the value by the given fittedvalue.

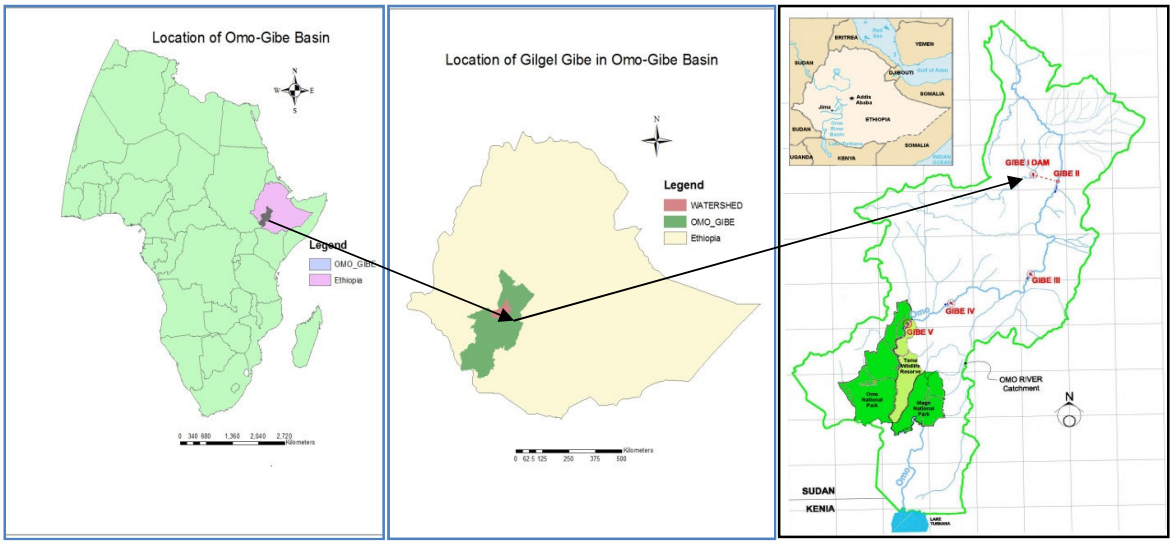

a) b) c)

Figure 1. Location map of Gilgel Gibe basin in Ethiopia.
Source for Fig.1c): http://www.internationalrivers.org/resources/maps-gibe-dam

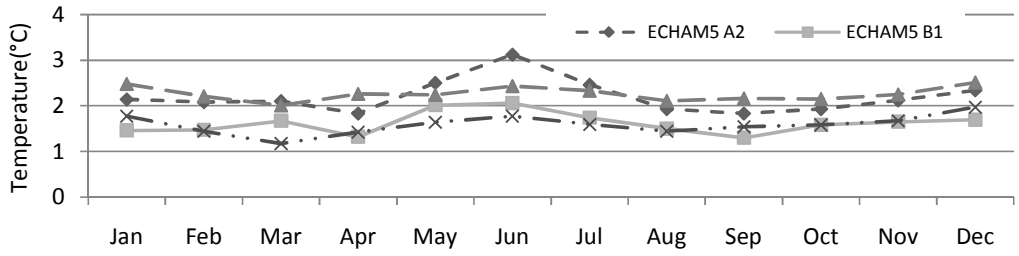

Figure 2. Future period 2050s temperature change in °C with respect to 1971 – 2000 baseline

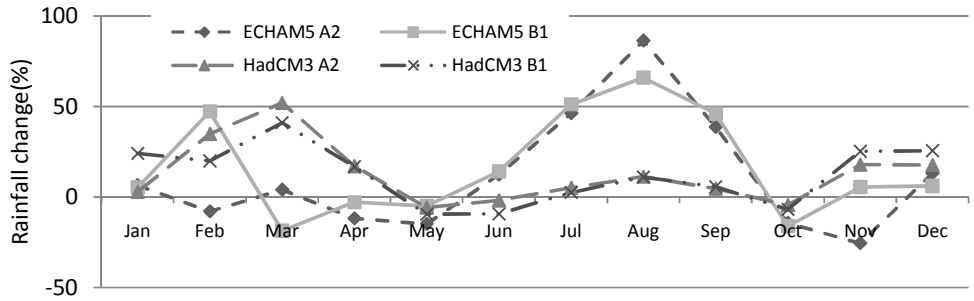

Figure 3. Future period 2050s rainfall change in % with respect to 1971 – 2000 baseline

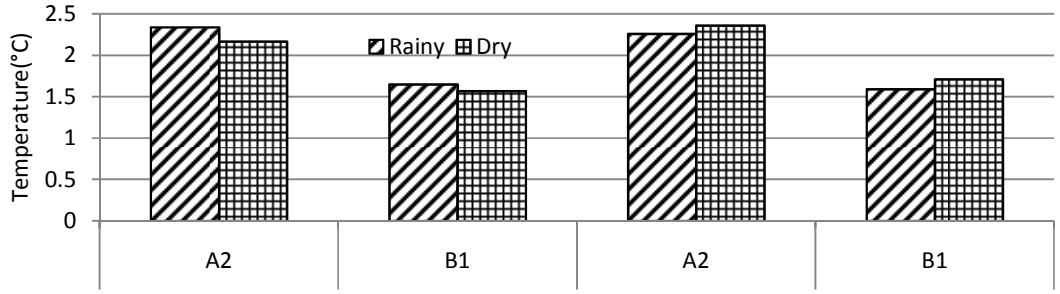

Figure 4. Future period 2050s seasonal temperature change in ° C with respect to 1971 – 2000 baseline

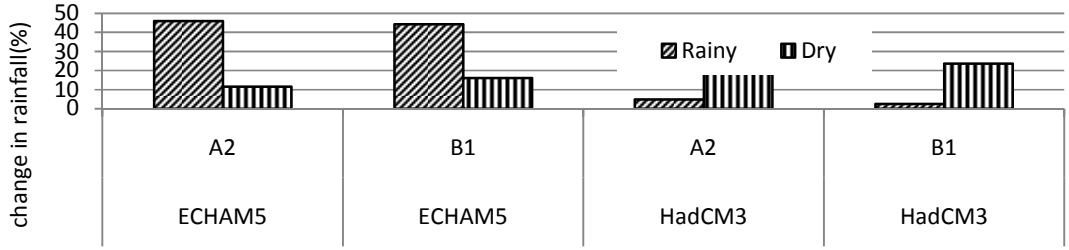

Figure 5.Future period 2050s seasonal rainfall change in % with respect to 1971 – 2000 baseline

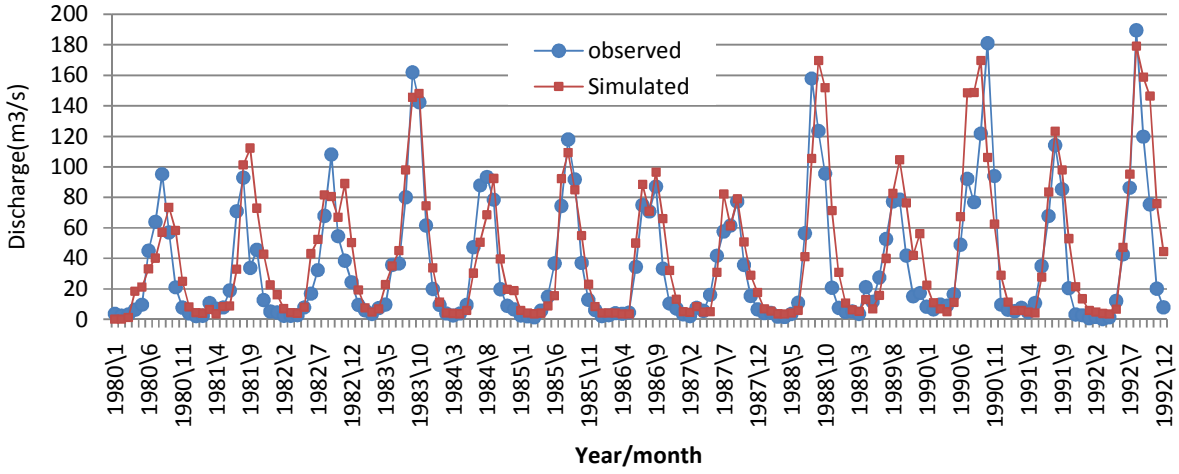

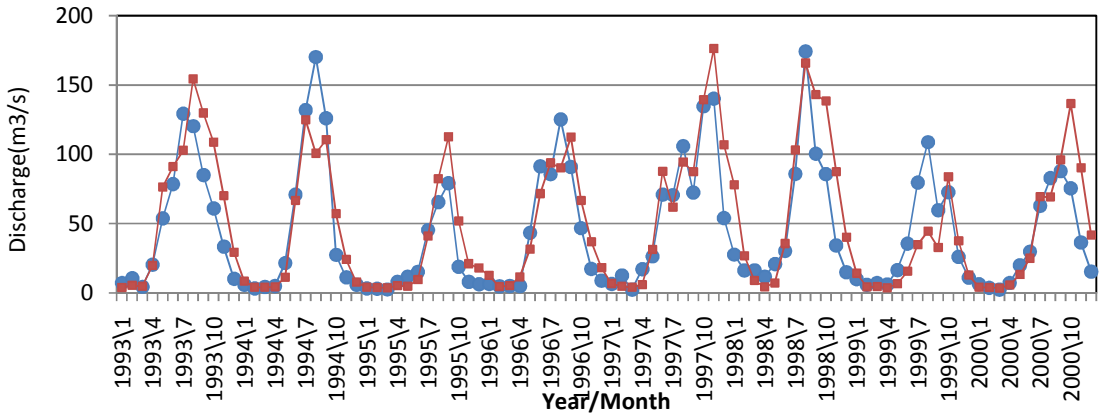

Figure 6. Monthly flow calibration (top) and monthly flow validation (bottom).

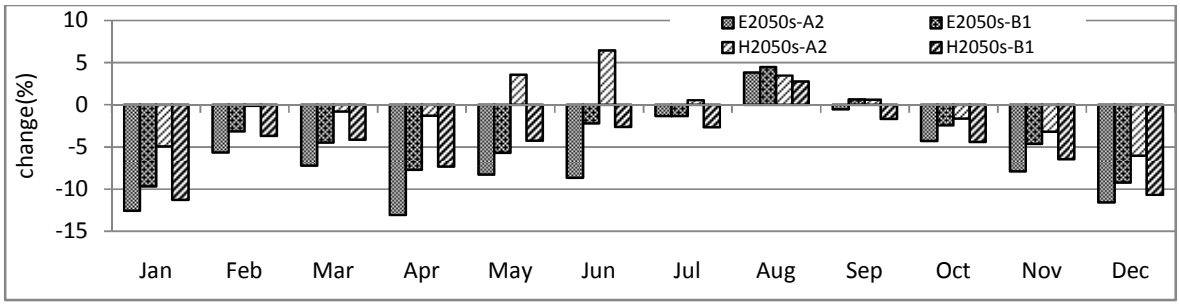

Figure 7. Percentage change in monthly streamflow.

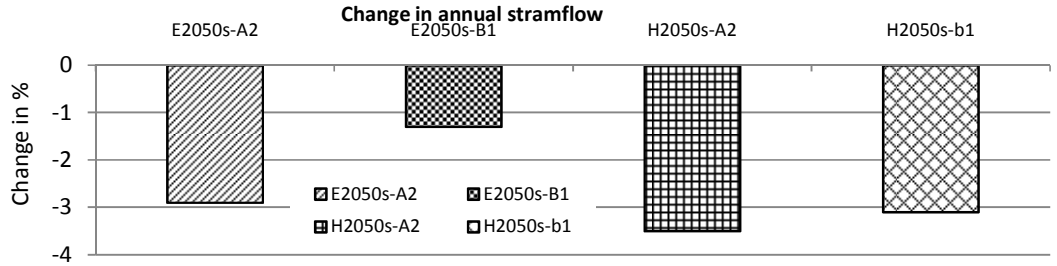

Figure 8. Percentage change in average annual streamflow

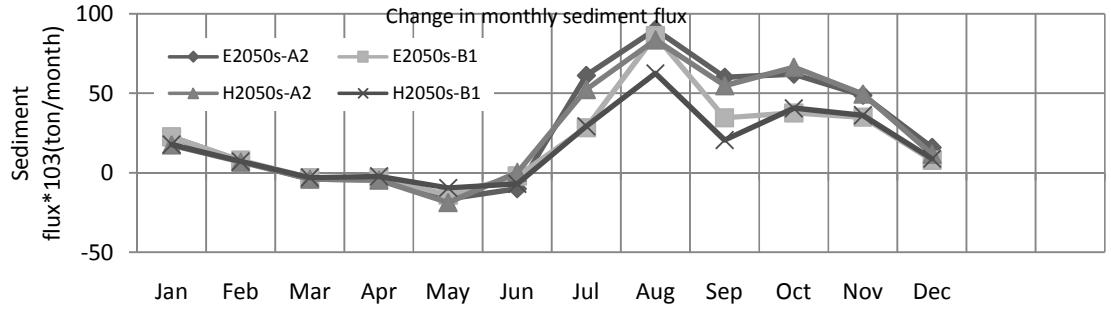

Figure 9. Percentage change in monthly sediment flux .

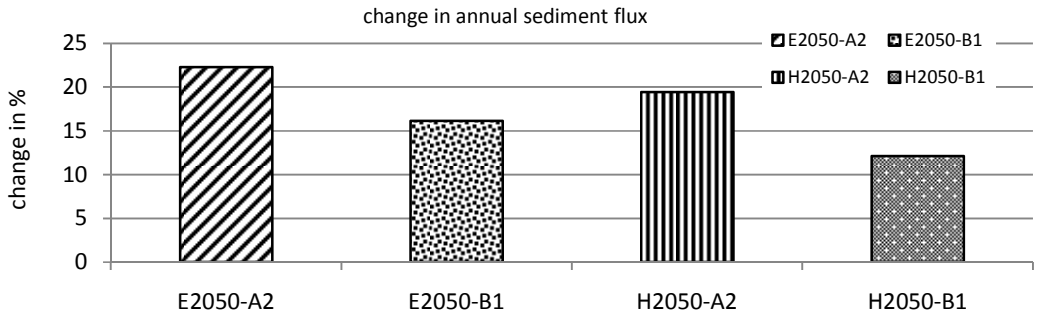

Figure 10. Percentage change in annual sediment.